Supporting Information

Missing Monometallofullerene with C_{80} Cage

Hidefumi Nikawa, Tomoya Yamada, Baopeng Cao, Naomi Mizorogi, Slanina Zdenek, Takahiro Tsuchiya, Takeshi Akasaka,* Kenji Yoza, Shigeru Nagase*

Center for Tsukuba Advanced Research Alliance, University of Tsukuba, Ibaraki 305-8577, Japan

Bruker AXS K. K., Yokohama 221-0022, Japan,

Institute for Molecular Science, Aichi 444-8585, Japan

Table of Contents

Supporting Information

References. The complete list of authors for citations.

(19) Frisch, M. J.; Trucks, G. W.; Schlegel, H. B.; Scuseria, G. E.; Robb, M. A.; Cheeseman, J. R.; Montgomery, Jr., J. A.; Vreven, T.; Kudin, K. N.; Burant, J. C.; Millam, J. M.; Iyengar, S. S.; Tomasi, J.; Barone, V.; Mennucci, B.; Cossi, M.; Scalmani, G.; Rega, N.; Petersson, G. A.; Nakatsuji, H.; Hada, M.; Ehara, M.; Toyota, K.; Fukuda, R.; Hasegawa, J.; Ishida, M.; Nakajima, T.; Honda, Y.; Kitao, O.; Nakai, H.; Klene, M.; Li, X.; Knox, J. E.; Hratchian, H. P.; Cross, J. B.; Adamo, C.; Jaramillo, J.; Gomperts, R.; Stratmann, R. E.; Yazyev, O.; Austin, A. J.; Cammi, R.; Pomelli, C.; Ochterski, J. W.; Ayala, P. Y.; Morokuma, K.; Voth, G. A.; Salvador, P.; Dannenberg, J. J.; Zakrzewski, V. G.; Dapprich, S.; Daniels, A. D.; Strain, M. C.; Farkas, O.; Malick, D. K.; Rabuck, A. D.; Raghavachari, K.; Foresman, J. B.; Ortiz, J. V.; Cui, Q.; Baboul, A. G.; Clifford, S.; Cioslowski, J.; Stefanov, B. B.; Liu, G.; Liashenko, A.; Piskorz, P.; Komaromi, I.; Martin, R. L.; Fox, D. J.; Keith, T.; Al-Laham, M. A.; Peng, C. Y.; Nanayakkara, A.; Challacombe, M.; Gill, P. M. W.; Johnson, B.; Chen, W.; Wong, M. W.; Gonzalez, C.; Pople, J. A. GAUSSIAN 03, Revision C. 01, Gaussian Inc., Wallingford, CT, 2004.

(25) Akasaka, T.; Wakahara, T; Nagase, S.; Kobayashi, K.; Waelchli, M.; Yamamoto, K.; Kondo, M.; Shirakura, S.; Okubo, S.; Maeda, Y.; Kato, T.; Kako, M.; Nakadaira, Y.; Nagahata, R.; Gao, X.; Caemelbecke, E. V.; Kadish, K. M. *J. Am. Chem. Soc.* **2000,** *122,* 9316-9317.

Supporting Information

Experimental detail

Spectra data of La@$C_{80}(C_6H_3Cl_2)$-A: Vis-near-IR (CS_2) $\lambda_{max}(\varepsilon)$ = 525 (7200), 620 (7200), 658 (8300), 1150 (900) nm. ^{1}H NMR (500 MHz, CS_2/acetone-d_6 (capillary)): δ 8.25 (d, J = 8.2 Hz, 1H), 7.15 (dd, J = 8.2, 2.2 Hz, 1H), 7.13 (d, J = 2.2 Hz, 1H) ppm. ^{13}C NMR (125 MHz, CS_2/acetone-d_6 (capillary)): δ 158.10 (s, 1C), 154.76 (s, 1C), 153.36 (s, 1C), 152.72 (s, 1C), 151.11 (s, 1C), 150.54 (s, 1C), 150.13 (s, 1C), 149.96 (s, 1C), 149.87 (s, 1C), 149.66 (s, 1C), 149.08 (s, 1C), 148.86 (s, 1C), 148.38 (s, 1C+1C), 147.94 (s, 1C), 147.64 (s, 1C), 146.24 (s, 1C), 146.15 (s, 1C), 145.45 (s, 1C), 145.14 (s, 1C+1C), 144.90 (s, 1C), 144.13 (s, 1C), 144.05 (s, 1C), 143.77 (s, 1C), 143.49 (s, 1C), 142.97 (s, 1C), 142.92 (s, 1C), 142.68 (s, 1C), 142.49 (s, 1C), 142.10 (s, 1C), 142.01 (s, 1C), 141.70 (s, 1C), 141.08 (s, 1C), 141.03 (s, 1C+1C), 140.53 (s, 1C), 140.38 (s, 1C), 140.33 (s, 1C), 140.32 (s, 1C), 140.30 (s, 1C), 139.95 (s, 1C), 139.64 (s, 1C), 139.13 (s, 1C), 138.29 (s, 1C), 137.98 (s, 1C), 137.89 (s, 1C), 137.74 (s, 1C), 137.56 (s, 1C), 137.34 (s, 1C), 137.07 (s, 1C), 136.92 (s, 1C), 136.85 (s, 1C), 136.59 (s, 1C), 136.57 (s, 1C), 136.52 (s, 1C), 135.87 (s, 1C), 135.42 (s, 1C), 135.04 (s, 1C), 134.68 (s, 1C), 134.47 (s, 1C), 134.45 (s, 1C), 133.57 (s, 1C), 133.13 (s, 1C), 132.98 (s, 1C), 132.92 (s, 1C), 132.81 (s, 1C), 132.56 (s, 1C), 132.42 (d, 1C), 132.28 (s, 1C), 131.60 (s, 1C), 131.56 (s, 1C), 131.34 (s, 1C), 130.99 (s, 1C), 130.81 (s, 1C), 130.54 (d, 1C), 130.21 (s, 1C), 129.36 (s, 1C), 129.05 (s, 1C), 128.51 (d, 1C), 127.01 (s, 1C), 125.32 (s, 1C), 124.55 (s, 1C), 96.45 (s, 1C), 89.16 (s, 1C), 59.00 (s, 1C) ppm. ^{139}La NMR (84.7 MHz, CS_2/acetone-d_6 (capillary)): δ -493 ppm. LD-TOF mass (positive and negative): m/z 1099 (La@C_{80}). MALDI-TOF mass (positive and negative, matrix: 1,1,4,4-tetraphenyl-1,3-butadiene): m/z 1244 (La@$C_{80}(C_6H_3Cl_2)$).

Black crystals were obtained by diffusion of hexane at room temperature into a solution of La@$C_{80}(C_6H_3Cl_2)$ in toluene, and the single-crystal X-ray diffraction data were collected on a Bruker SMART APEX-II URTRA equipped with a CCD area detector using Mo-K . Crystal data for a black needle of La@$C_{80}(C_6H_3Cl_2)\cdot1.5(C_7H_8)$: MF = $C_{96.50}H_{15}C_{l2}La$, FW = 1383.90, 0.18 mm × 0.12 mm × 0.07 mm, monoclinic, *P21/c* (no. 14), a = 11.5336(16) Å, b = 22.057(3) Å, c =

20.237(3) Å, β = 105.548(2)°, V = 4959.8(12) Å, Z = 4, Dcalcd = 1.853 g cm^{-3}, μ(Mo Ka)) 1.038 mm^{-1}. An empirical absorption correction (0.8351 ≤ T ≤ 0.9309), π and ω scan, θ = 1.39-27.49°, T = 90 K, 54901 refractions collected (11248 independent Rint = 0.0520), R1 = 0.1155, wR2 = 0.2390 for all data, R_1 = 0.0983, wR_2 = 0.2288 for 9123 reflections (I > 2.0σ(I)) and 1196 parameters, GOF on F^2 = 1.118. The maximum and minimum residual electron density is equal to 1.211 and -0.894 e $Å^{-3}$, respectively. These relatively high R values are due to general disorder of La atom and all La@C_{80}($C_6H_3Cl_2$) cage carbons.

Spectra data of La@C_{80}($C_6H_3Cl_2$)-B: Vis-near-IR (CS_2) λ_{max} = 525, 620, 658, 1151 nm. ^{1}H NMR (500 MHz, CS_2/acetone-d_6 (capillary)): δ 8.28 (d, J = 2.5 Hz, 1H), 7.08 (d, J = 8.5 Hz, 1H), 6.97 (dd, J = 8.5, 2.5 Hz, 1H) ppm. ^{13}C NMR (125 MHz, CS_2/acetone-d_6 (capillary)): δ 158.13 (s, 1C), 154.82 (s, 1C), 153.41 (s, 1C), 152.76 (s, 1C), 151.15 (s, 1C), 150.60 (s, 1C), 150.16 (s, 1C), 150.00 (s, 1C), 149.92 (s, 1C), 149.71 (s, 1C), 149.11 (s, 1C), 148.92 (s, 1C), 148.42 (s, 1C+1C), 147.98 (s, 1C), 147.70 (s, 1C), 146.29 (s, 1C), 146.20 (s, 1C), 145.50 (s, 1C), 145.19 (s, 1C), 145.18 (s, 1C), 144.96 (s, 1C), 144.17 (s, 1C), 144.12 (s, 1C), 143.86 (s, 1C), 143.55 (s, 1C), 143.46 (s, 1C), 143.00 (s, 1C+1C), 142.78 (s, 1C), 142.54 (s, 1C), 142.15 (s, 1C), 142.05 (s, 1C), 141.73 (s, 1C), 141.14 (s, 1C), 141.08 (s, 1C), 141.07 (s, 1C), 140.46 (s, 1C), 140.37 (s, 1C), 140.35 (s, 1C+1C), 139.99 (s, 1C), 139.68 (s, 1C), 139.17 (s, 1C), 138.34 (s, 1C), 138.02 (s, 1C), 137.95 (s, 1C), 137.81 (s, 1C), 137.60 (s, 1C), 137.41 (s, 1C), 137.12 (s, 1C), 136.90 (s, 1C), 136.61 (s, 1C), 136.56 (s, 1C), 136.35 (s, 1C), 135.48 (s, 1C), 135.36 (s, 1C), 135.06 (s, 1C), 134.73 (s, 1C), 134.53 (s, 1C), 134.46 (s, 1C), 133.67 (s, 1C), 133.66 (d, 1C), 133.39 (s, 1C), 133.19 (s, 1C), 133.05 (s, 1C), 132.97 (s, 1C), 132.86 (s, 1C), 132.59 (s, 1C), 132.33 (s, 1C), 131.64 (s, 1C), 131.61 (s, 1C), 131.39 (s, 1C), 131.14 (s, 1C), 130.89 (d, 1C), 130.86 (s, 1C), 130.23 (s, 1C), 130.01 (d, 1C), 129.42 (s, 1C), 129.10 (s, 1C), 127.09 (s, 1C), 125.36 (s, 1C), 124.59 (s, 1C), 96.20 (s, 1C), 88.93 (s, 1C), 59.22 (s, 1C) ppm. ^{139}La NMR (84.7 MHz, CS_2/acetone-d_6 (capillary)): δ -500 ppm. LD-TOF mass (positive

and negative mode): m/z 1099 ($La@C_{80}$). MALDI-TOF mass (positive and negative mode, matrix: 1,1,4,4-tetraphenyl-1,3-butadiene): m/z 1244 ($La@C_{80}(C_6H_3Cl_2)$).

Spectra data of $La@C_{80}(C_6H_3Cl_2)$-C: Vis-near-IR (CS_2) λ_{max} = 526, 657, 1162 nm. ^{1}H NMR (500 MHz, CS_2/acetone-d_6 (capillary)): δ 8.82 (d, J = 2.5 Hz, 1H), 8.68 (dd, J = 8.5, 2.5 Hz, 1H), 8.02 (d, J = 8.5 Hz, 1H) ppm. ^{13}C NMR (125 MHz, CS_2/acetone-d_6 (capillary)): δ 157.86 (s, 1C), 154.42 (s, 1C), 153.01 (s, 1C), 152.45 (s, 1C), 151.05 (s, 1C), 150.11 (s, 1C), 149.82 (s, 1C), 149.65 (s, 1C), 149.29 (s, 1C), 148.74 (s, 1C), 148.50 (s, 1C), 148.50 (s, 1C), 148.22 (s, 1C), 148.02 (s, 1C), 147.60 (s, 1C), 147.34 (s, 1C), 146.10 (s, 1C), 146.10 (s, 1C), 145.85 (s, 1C), 145.20 (s, 1C), 144.84 (s, 1C), 144.80 (s, 1C), 144.73 (s, 1C), 143.85 (s, 1C), 143.75 (s, 1C), 143.26 (s, 1C), 142.55 (s, 1C), 142.46 (s, 1C), 142.35 (s, 1C), 141.79 (s, 1C), 141.75 (s, 1C), 141.70 (s, 1C), 140.86 (s, 1C), 140.85 (s, 1C), 140.85 (s, 1C), 140.18 (s, 1C), 139.91 (s, 1C), 139.89 (s, 1C), 139.85 (s, 1C), 139.70 (s, 1C), 139.33 (s, 1C), 138.93 (s, 1C), 138.38 (s, 1C), 138.08 (s, 1C), 137.84 (s, 1C), 137.68 (s, 1C), 137.46 (s, 1C), 137.45 (s, 1C), 136.90 (s, 1C), 136.85 (s, 1C), 136.78 (s, 1C), 136.37 (s, 1C), 136.16 (s, 1C), 135.69 (s, 1C), 135.15 (s, 1C), 134.49 (s, 1C), 134.46 (s, 1C), 134.08 (s, 1C), 133.95 (s, 1C), 133.89 (s, 1C), 133.89 (s, 1C), 133.70 (s, 1C), 132.63 (s, 1C), 132.57 (s, 1C), 132.51 (s, 1C), 132.19 (d, 1C), 132.01 (s, 1C), 131.35 (s, 1C), 131.21 (s, 1C), 131.15 (s, 1C), 130.68 (s, 1C), 130.10 (s, 1C), 129.39 (s, 1C), 129.10 (s, 1C), 128.84 (s, 1C), 128.68 (s, 1C), 128.50 (d, 1C), 126.57 (s, 1C), 125.98 (d, 1C), 125.53 (s, 1C), 124.28 (s, 1C), 95.71 (s, 1C), 91.61 (s, 1C), 57.77 (s, 1C) ppm. ^{139}La NMR (84.7 MHz, CS_2/acetone-d_6 (capillary)): δ -488 ppm. LD-TOF mass (positive and negative mode): m/z 1099 ($La@C_{80}$). MALDI-TOF mass (positive and negative mode, matrix: 1,1,4,4-tetraphenyl-1,3-butadiene): m/z 1244 ($La@C_{80}(C_6H_3Cl_2)$).

Supporting Information

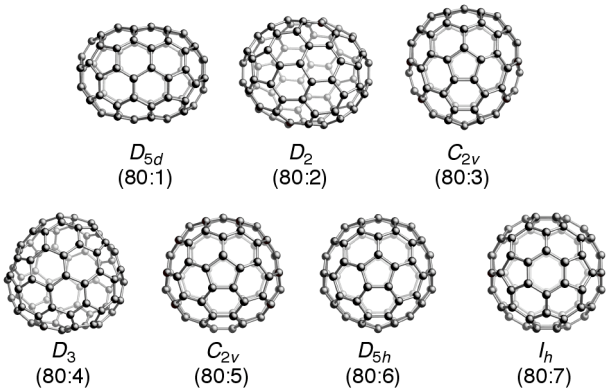

Figure S1. Seven IPR-satisfying isomers of C_{80} cage.

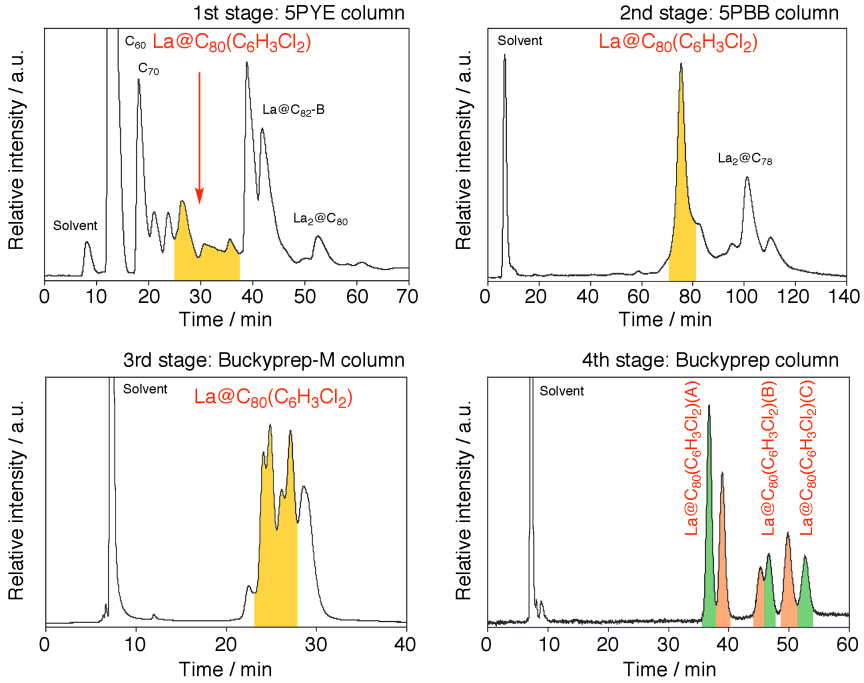

Figure S2. Four stage HPLC profiles for isolation of $La@C_{80}(C_6H_3Cl_2)$(A-C).

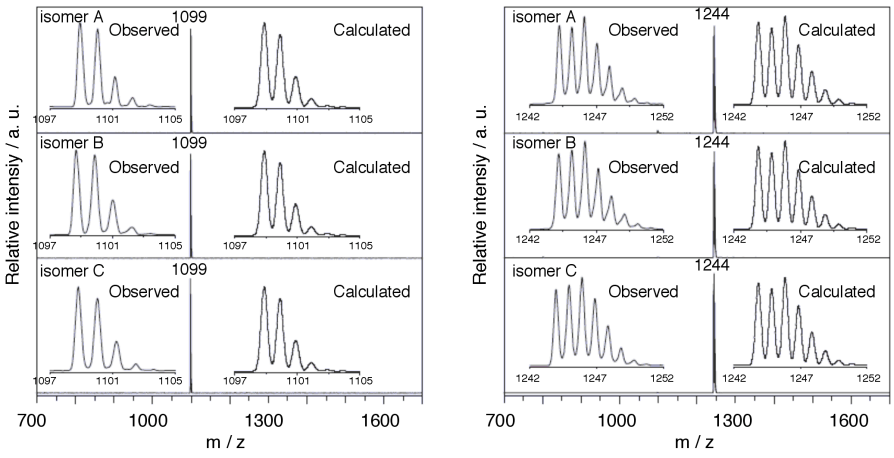

Figure S3. LD-TOF and MALDI-TOF mass spectra of $La@C_{80}(C_6H_3Cl_2)$ (A-C).

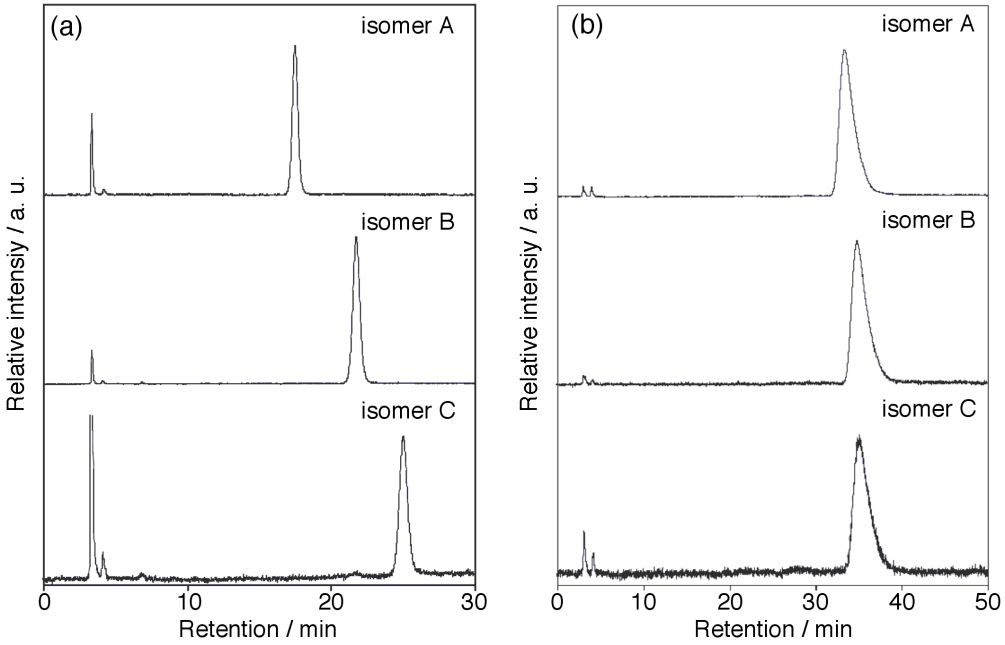

(a) Buckyprep column (ϕ 4.6 × 250 mm), toluene (1.0 mL/min), UV detector (330 nm)
(b) 5PBB column (ϕ 4.6 × 250 mm), toluene (1.0 mL/min), UV detector (330 nm)

Figure S4. HPLC profiles of isolated La@C_{80}($C_6H_3Cl_2$)(A-C) by (a) Buckyprep and (b) 5PBB column.

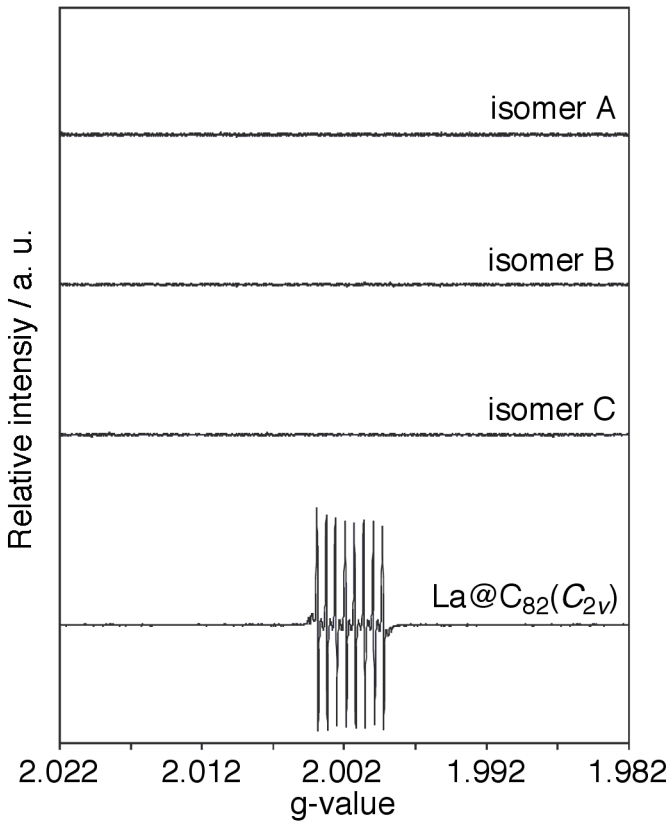

Figure S5. EPR spectra of La@C_{80}($C_6H_3Cl_2$)(A-C) and La@C_{82}(C_{2v}).

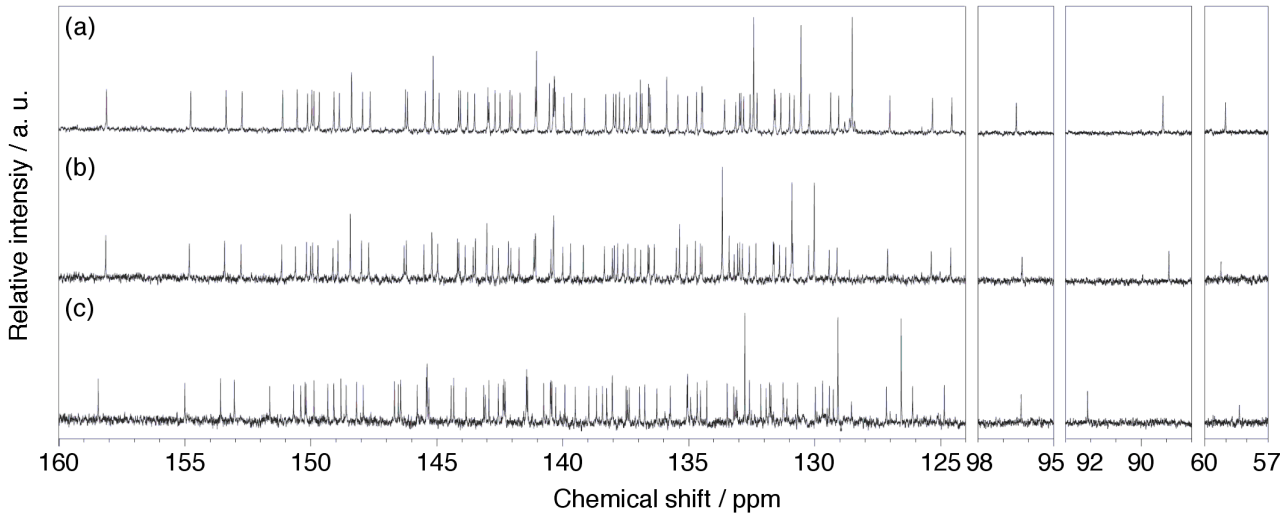

Figure S6. Vis-near-IR spectra of (a) La@$C_{80}C_6H_3Cl_2$(A), (b) La@$C_{80}C_6H_3Cl_2$(B), and (c) La@$C_{80}C_6H_3Cl_2$(C) in CS_2.

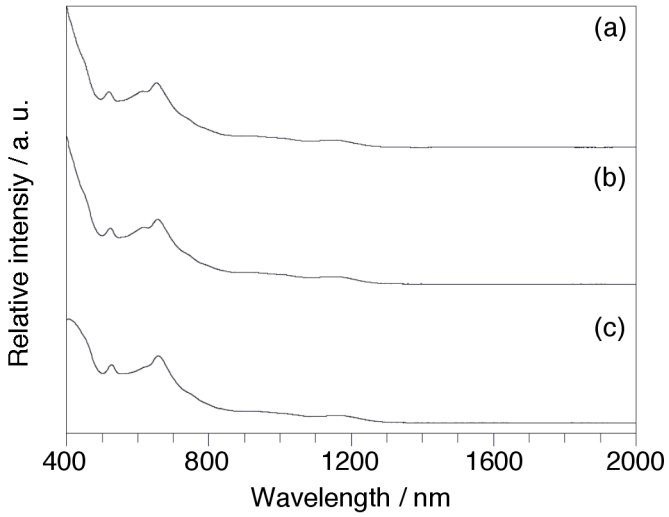

Figure S7. ^{13}C NMR spectra of (a) La@$C_{80}C_6H_3Cl_2$(A), (b) La@$C_{80}C_6H_3Cl_2$(B), and (c) La@$C_{80}C_6H_3Cl_2$(C) measured at 125 MHz on a Bruker AVANCE 500 spectrometer with a CryoProbe system in CS_2 (acetone-d_6 in capillary as lock solvent).

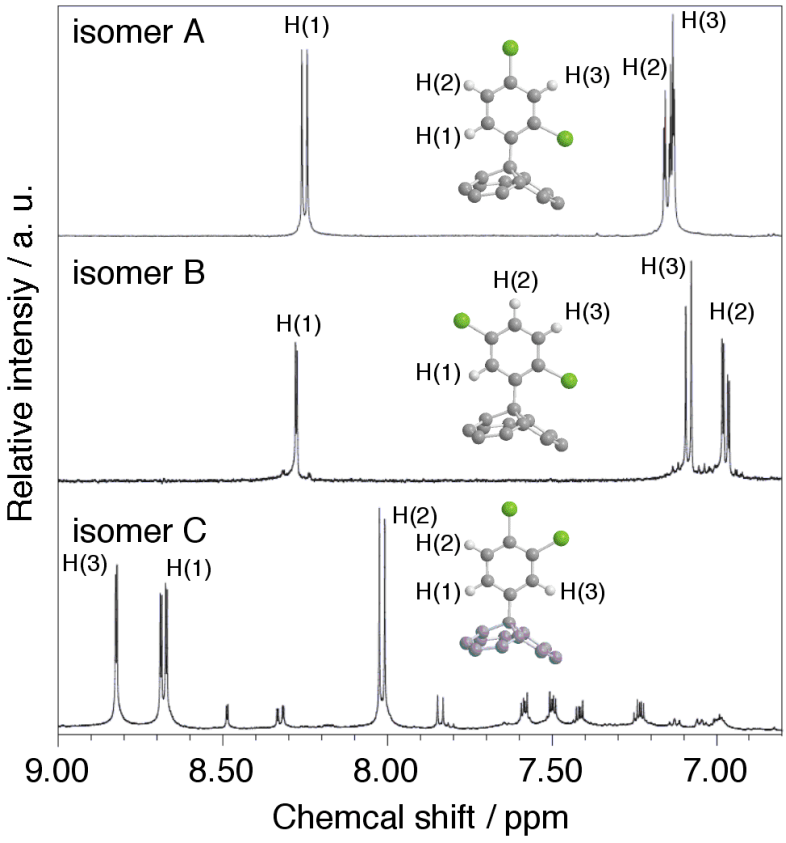

Figure S8. ^{1}H NMR spectra of La@C_{80}($C_6H_3Cl_2$)(A-C).

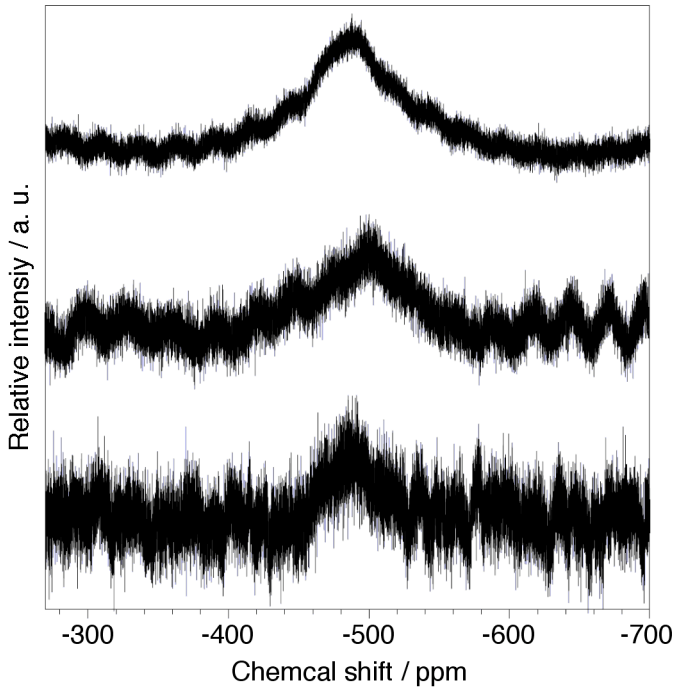

Figure S9. ^{139}La NMR spectra of La@C_{80}($C_6H_3Cl_2$)(A-C).

Supporting Information

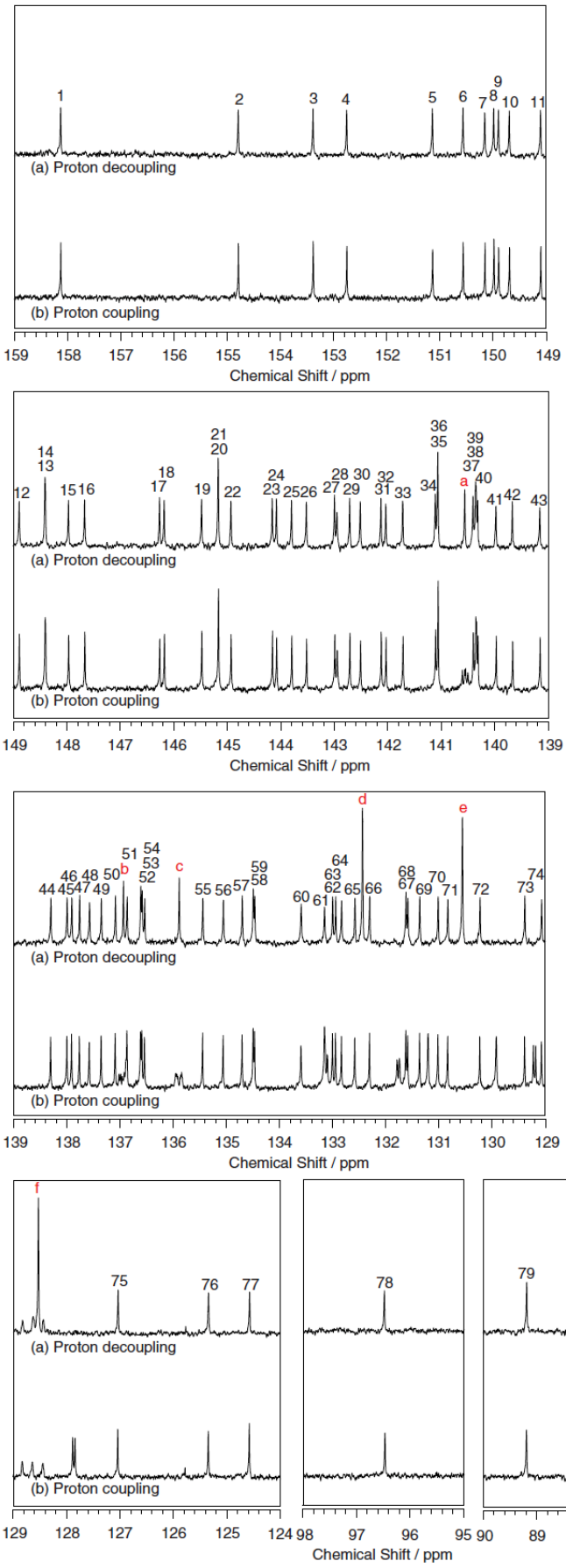

Fullerene cage

	Chemical shift (ppm)		Chemical shift (ppm)
1	158.10	41	139.95
2	154.76	42	139.64
3	153.36	43	139.13
4	152.72	44	138.29
5	151.11	45	137.98
6	150.54	46	137.89
7	150.13	47	137.74
8	149.96	48	137.56
9	149.87	49	137.34
10	149.66	50	137.07
11	149.08	51	136.85
12	148.86	52	136.59
13	148.38	53	136.57
14	148.38	54	136.52
15	147.94	55	135.42
16	147.64	56	135.04
17	146.24	57	134.68
18	146.15	58	134.47
19	145.45	59	134.45
20	145.14	60	133.57
21	145.14	61	133.13
22	144.90	62	132.98
23	144.13	63	132.92
24	144.05	64	132.81
25	143.77	65	132.56
26	143.49	66	132.28
27	142.97	67	131.60
28	142.92	68	131.56
29	142.68	69	131.34
30	142.49	70	130.99
31	142.10	71	130.81
32	142.01	72	130.21
33	141.70	73	129.36
34	141.08	74	129.05
35	141.03	75	127.01
36	141.03	76	125.32
37	140.38	77	124.55
38	140.33	78	96.45
39	140.32	79	89.16
40	140.30	80	59.00

Dichlorophenyl group

	Chemical shift (ppm)		Chemical shift (ppm)
a	140.53	d	132.42
b	136.92	e	130.54
c	135.87	f	128.51

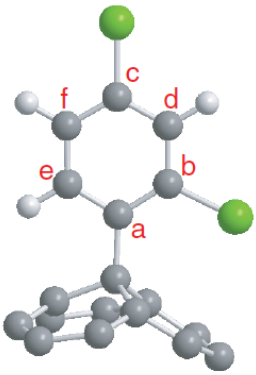

Figure S10. ^{13}C NMR spectra of La@C_{80}($C_6H_3Cl_2$)(A)

Supporting Information

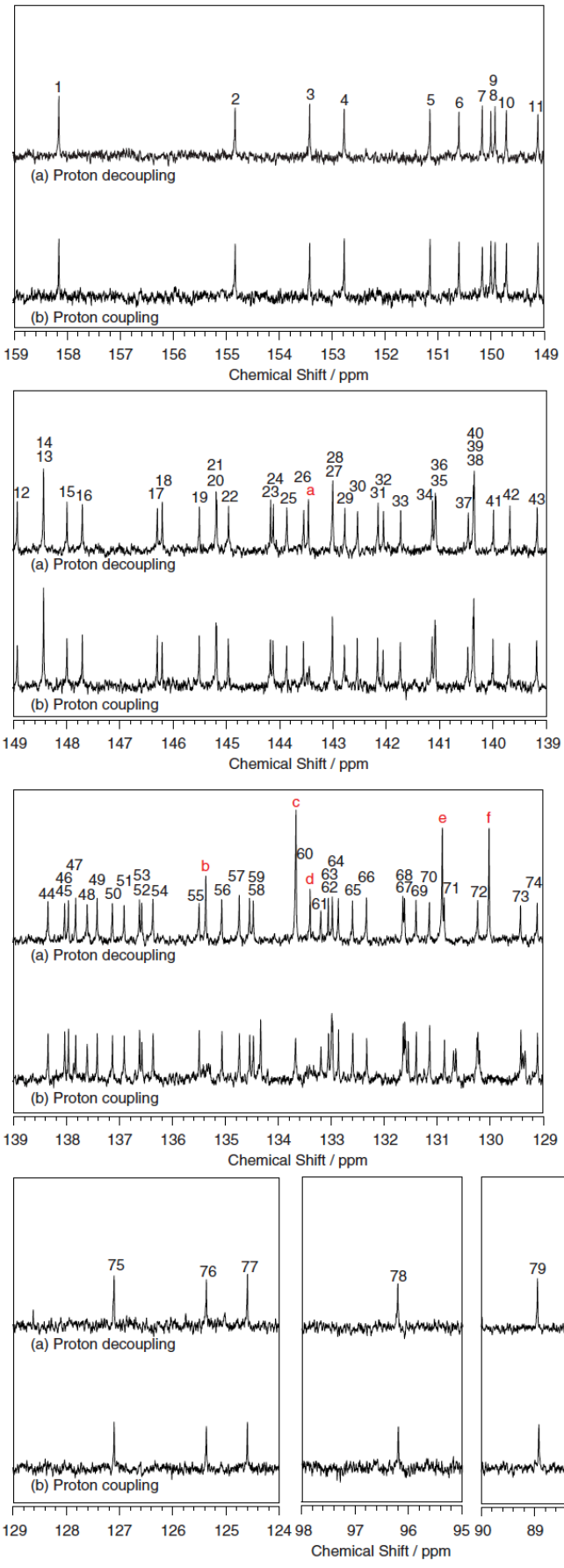

Fullerene cage

	Chemical shift (ppm)		Chemical shift (ppm)
1	158.13	41	139.99
2	154.82	42	139.68
3	153.41	43	139.17
4	152.76	44	138.34
5	151.15	45	138.02
6	150.60	46	137.95
7	150.16	47	137.81
8	150.00	48	137.60
9	149.92	49	137.41
10	149.71	50	137.12
11	149.11	51	136.90
12	148.92	52	136.61
13	148.42	53	136.56
14	148.42	54	136.35
15	147.98	55	135.48
16	147.70	56	135.06
17	146.29	57	134.73
18	146.20	58	134.53
19	145.50	59	134.46
20	145.19	60	133.67
21	145.18	61	133.19
22	144.96	62	133.05
23	144.17	63	132.97
24	144.12	64	132.86
25	143.86	65	132.59
26	143.55	66	132.33
27	143.00	67	131.64
28	143.00	68	131.61
29	142.78	69	131.39
30	142.54	70	131.14
31	142.15	71	130.86
32	142.05	72	130.23
33	141.73	73	129.42
34	141.14	74	129.10
35	141.08	75	127.09
36	141.07	76	125.36
37	140.46	77	124.59
38	140.37	78	96.20
39	140.35	79	88.93
40	140.35	80	59.22

Dichlorophenyl group

	Chemical shift (ppm)		Chemical shift (ppm)
a	143.46	d	133.39
b	135.36	e	130.89
c	133.66	f	130.01

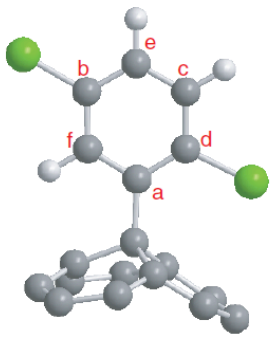

Figure S11. ^{13}C NMR spectra of La@$C_{80}(C_6H_3Cl_2)$(B).

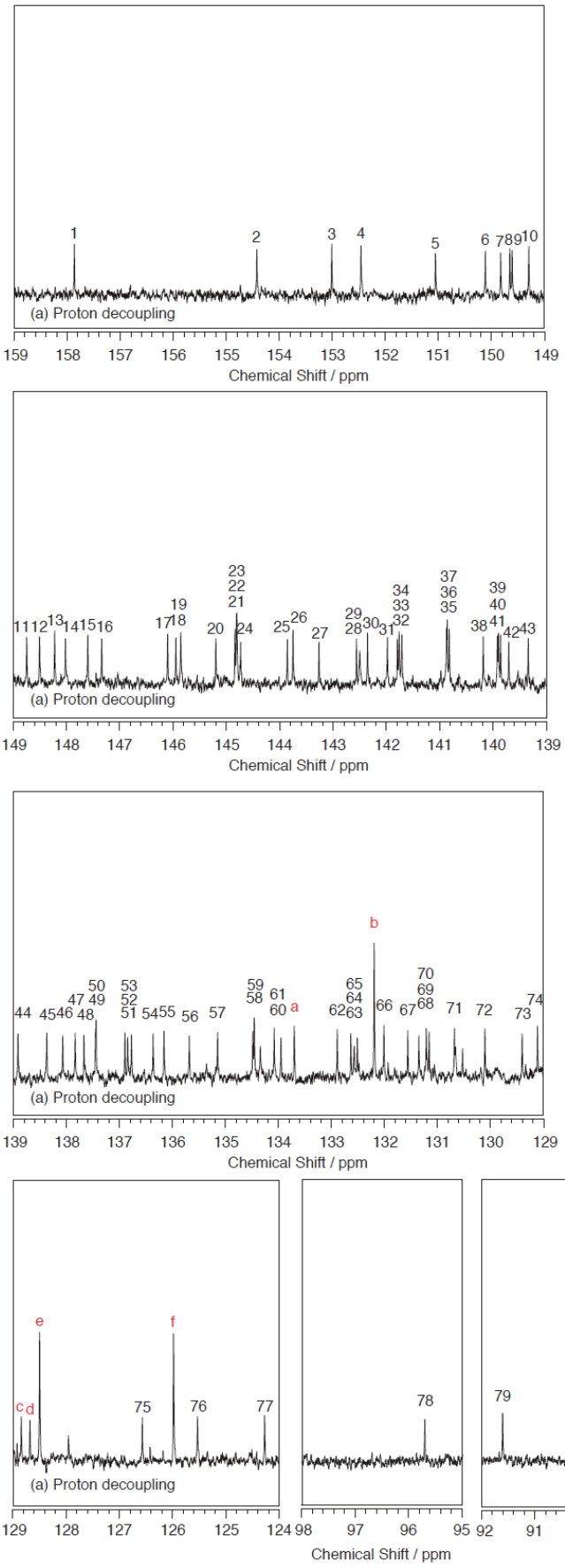

Fullerene cage

	Chemical shift (ppm)		Chemical shift (ppm)
1	157.86	41	139.85
2	154.42	42	139.70
3	153.01	43	139.33
4	152.45	44	138.93
5	151.05	45	138.38
6	150.11	46	138.08
7	149.82	47	137.84
8	149.65	48	137.68
9	149.60	49	137.46
10	149.29	50	137.45
11	148.74	51	136.90
12	148.50	52	136.85
13	148.22	53	136.78
14	148.02	54	136.37
15	147.60	55	136.16
16	147.34	56	135.69
17	146.10	57	135.15
18	145.95	58	134.49
19	145.85	59	134.46
20	145.20	60	134.08
21	144.84	61	133.95
22	144.81	62	132.89
23	144.80	63	132.63
24	144.73	64	132.57
25	143.85	65	132.51
26	143.75	66	132.01
27	143.26	67	131.55
28	142.55	68	131.35
29	142.49	69	131.21
30	142.35	70	131.15
31	141.97	71	130.68
32	141.79	72	130.10
33	141.75	73	129.39
34	141.70	74	129.10
35	140.86	75	126.57
36	140.85	76	125.53
37	140.81	77	124.28
38	140.18	78	95.71
39	139.91	79	91.61
40	139.89	80	57.77

Dichlorophenyl group

	Chemical shift (ppm)		Chemical shift (ppm)
a	133.70	d	128.68
b	132.19	e	128.50
c	128.84	f	125.98

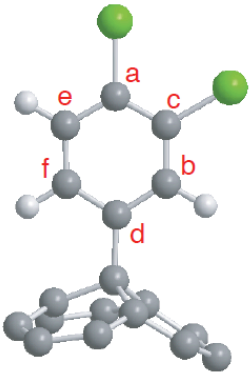

Figure S12. ^{13}C NMR spectra of La@$C_{80}(C_6H_3Cl_2)(C)$.

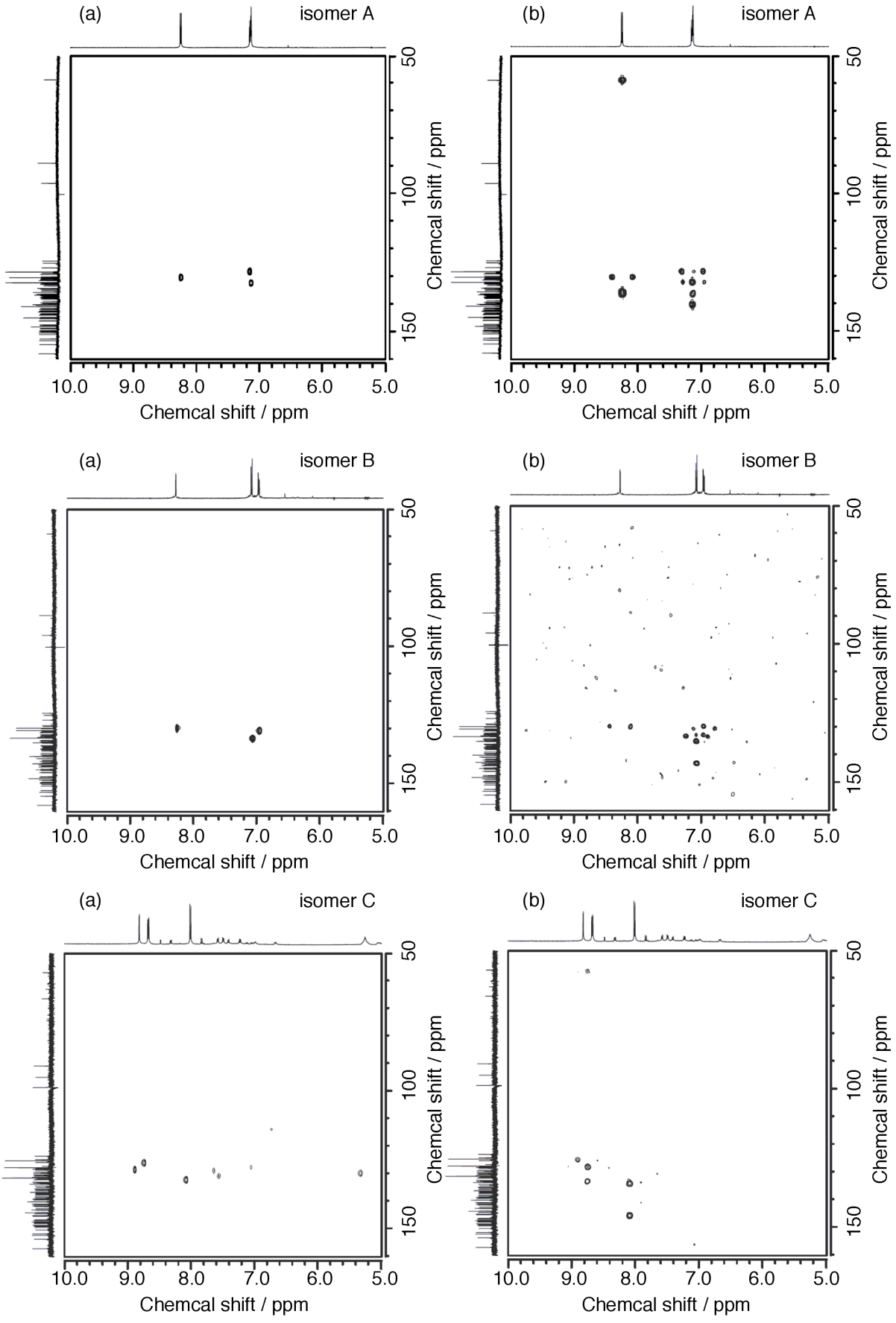

Figure S13. (a) HMQC and (b) HMBC spectra of La@$C_{80}(C_6H_3Cl_2)$(A-C).

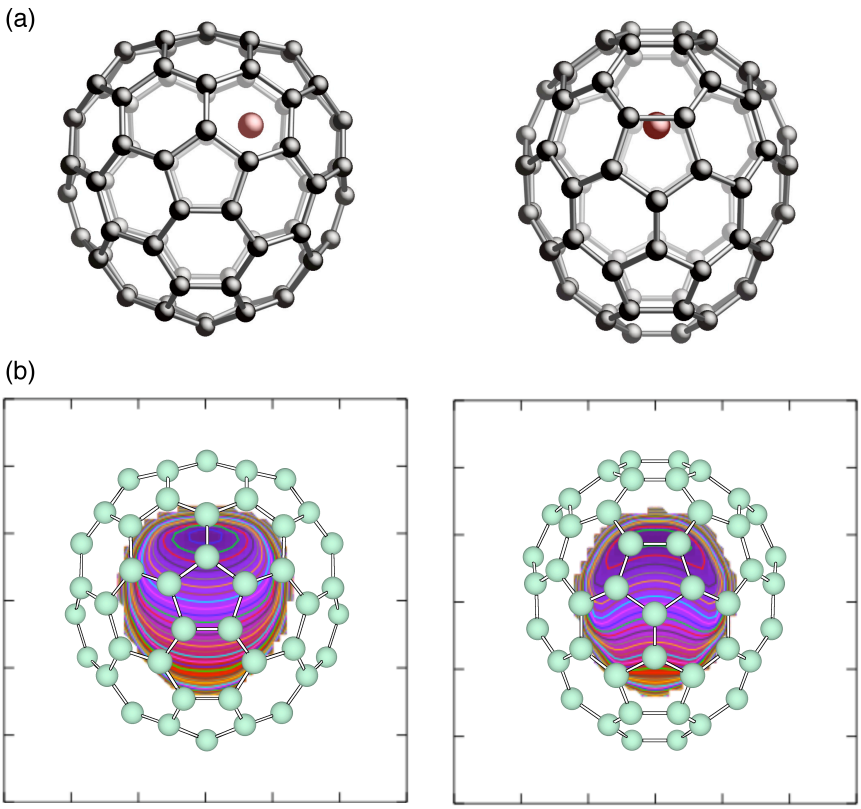

Figure S14. Two views of (a) the optimized structure and (b) the electrostatic potential map inside of $[C_{80}]^{3-}$.

Table 1. Redox Potentials (V)[a] of La@C_{80}($C_6H_3Cl_2$)(A-C).

Compound	$^{ox}E_2$	$^{ox}E_1$	$^{red}E_1$	$^{red}E_2$	$^{red}E_3$
La@C_{80}($C_6H_3Cl_2$)(A)	-	+0.31	-1.09	-1.42	-1.95
La@C_{80}($C_6H_3Cl_2$)(B)	+0.81	+0.36	-1.07	-1.43	-1.89
La@C_{80}($C_6H_3Cl_2$)(C)	+0.75	+0.35	-1.05	-1.41	-1.86

[a] Versus Fc/Fc^+. In 1,2-dichlorobezene with 0.1 M (n-Bu)$_4$NPF$_6$ at a Pt working electrode. CV: scan rate, 20 m·s^{-1}.

Table 2. Calculated ^{13}C NMR chemical shift and xyz coordinates of La@$C_{80}(C_6H_3Cl_2)$(A).

Atoms	Calculated ^{13}C NMR chemical shift	Coordinates		
		X	y	y
C (1)	58.85	-3.552441	0.025575	-0.097080
C (2)	85.20	-2.914508	-0.152364	-1.518786
C (3)	94.98	-2.97174	-1.094799	0.741097
C (4)	141.69	-2.306421	1.062902	-1.955199
C (5)	125.95	-5.740267	-0.027349	-1.375530
C (6)	130.77	-2.439335	2.039815	-0.884102
C (7)	136.37	-2.822795	1.350365	0.319342
C (8)	142.70	0.702799	-2.870479	2.845528
C (9)	134.95	-1.507095	-2.022646	2.291087
C (10)	130.94	-2.296741	-0.856672	1.995206
C (11)	130.69	-2.301898	-2.568998	-1.175457
C (12)	129.32	-2.442136	-1.387775	-2.024251
C (13)	125.22	-1.321603	-1.369031	-2.959365
C (14)	140.13	-0.53041	-2.554869	-2.726167
C (15)	137.53	-1.079878	-3.255619	-1.578391
C (16)	137.75	-1.593246	3.113245	-0.846432
C (17)	141.60	-1.057896	3.568892	0.407767
C (18)	140.96	-2.579245	-2.397135	0.241860
C (19)	124.96	-1.617359	-2.952991	1.185000
C (20)	144.36	1.199642	4.322866	1.008201
C (21)	138.24	1.102823	3.529844	2.219918
C (22)	144.06	2.429935	3.034195	2.528922
C (23)	150.24	3.339095	3.530193	1.512524
C (24)	159.17	2.577213	4.297029	0.546321
C (25)	154.48	2.842165	4.157116	-0.815039
C (26)	148.14	3.885438	3.242953	-1.254159
C (27)	144.57	3.415819	2.532010	-2.419321
C (28)	142.06	2.079353	3.030195	-2.727025
C (29)	145.78	1.745515	4.045621	-1.757068
C (30)	149.46	4.384023	2.723194	1.098803
C (31)	146.19	4.623849	1.444775	1.738439
C (32)	139.98	5.206456	0.581492	0.735318
C (33)	145.93	5.081348	1.211328	-0.563219
C (34)	150.56	4.669266	2.577435	-0.326004
C (35)	140.10	5.113357	-0.773046	0.854941
C (36)	148.38	4.427109	-1.358852	1.983806
C (37)	152.60	4.007717	-2.686937	1.566975
C (38)	150.30	4.298014	-2.832684	0.151739
C (39)	140.49	0.154403	4.310479	0.106122
C (40)	147.92	2.867367	-3.256638	2.104800
C (41)	151.70	0.42929	4.163883	-1.322231
C (42)	142.79	-0.603206	3.339719	-1.891961
C (43)	138.45	0.620307	-3.798215	1.713767
C (44)	155.91	1.968914	-4.030879	1.265919
C (45)	149.54	2.24162	-4.169012	-0.094595
C (46)	141.33	1.172439	-4.077142	-1.059023

C (47)	140.80	1.704676	-3.407320	-2.236194
C (48)	145.68	3.073227	-3.010858	-1.958043
C (49)	149.55	3.416291	-3.533822	-0.660544
C (50)	138.35	-0.764667	0.498171	3.301677
C (51)	132.57	0.001138	-0.688637	3.651108
C (52)	139.63	1.372215	-0.303651	3.802184
C (53)	142.33	1.451375	1.128984	3.620878
C (54)	139.42	0.14491	1.620564	3.323022
C (55)	136.59	0.646801	-0.223196	-3.823464
C (56)	143.74	1.529238	0.899891	-3.709724
C (57)	149.73	2.843936	0.407784	-3.405537
C (58)	143.42	2.780551	-1.022377	-3.321824
C (59)	137.40	1.434369	-1.422235	-3.615415
C (60)	123.93	-1.853799	0.446668	2.422957
C (61)	129.44	-2.090211	1.587072	1.498456
C (62)	129.05	-1.174363	2.747450	1.551643
C (63)	129.78	-0.049243	2.753887	2.494647
C (64)	130.57	2.618502	1.759151	3.119753
C (65)	135.89	3.747513	0.913559	2.711932
C (66)	137.01	3.647887	-0.554783	2.845465
C (67)	134.05	2.43016	-1.160111	3.412079
C (68)	135.64	-0.696822	-0.141848	-3.389294
C (69)	131.19	-1.193507	1.126312	-2.851321
C (70)	132.55	-0.305911	2.303335	-2.806603
C (71)	129.16	1.084836	2.168757	-3.252404
C (72)	133.33	3.755611	1.172689	-2.630835
C (73)	136.21	4.612324	0.466385	-1.670417
C (74)	137.18	4.515481	-1.004629	-1.544796
C (75)	134.31	3.582183	-1.754955	-2.399833
C (76)	127.10	-0.335766	-1.948728	3.103624
C (77)	131.59	-0.462075	-3.750108	0.799757
C (78)	127.09	-0.179103	-3.903075	-0.644620
C (79)	130.88	0.870271	-2.582389	-3.021192
C (80)	140.13	-5.089047	0.134083	-0.142885
C (81)	143.49	-5.900053	0.374942	0.974317
C (82)	127.90	-7.288132	0.453176	0.879971
C (83)	147.37	4.888644	-1.599038	-0.316111
C (84)	143.95	-7.887144	0.285215	-0.362637
C (85)	123.83	-7.125778	0.044048	-1.500070
C (86)	140.16	2.076095	-2.500000	3.048502
La (1)	-	-0.543129	-0.881787	-0.272599
H (1)	-	-5.141511	-0.215223	-2.257857
H (2)	-	-7.602963	-0.086164	-2.461840
H (3)	-	-7.88373	0.642433	1.761800
Cl (1)	-	-5.211768	0.605211	2.604370
Cl (2)	-	-9.661848	0.382595	-0.489736

* Calculated at the B3LYP-GIAO/6-311G(d)//B3LYP/3-21G(d) level.

Table 3. Crystal data and structure refinement of La@$C_{80}(C_6H_3Cl_2)$(A).

Empirical formula	$C_{96.50}\ H_{15}\ Cl_2\ La$	
Formula weight	1383.90	
Temperature	90 K	
Wavelength	0.71073 Å	
Crystal system	Monoclinic	
Space group	$P2_1/c$ (no. 14)	
Unit cell dimensions	a = 11.5336(16) Å	α = 90°
	b = 22.057(3) Å	β = 105.548(2)°
	c = 20.237(3) Å	γ = 90°
Volume	4959.8(12) $Å^3$	
Z	4	
Density (calculated)	1.853 g/m^3	
Absorption coefficient	1.038 mm^{-1}	
F (000)	2740	
Crystal size	0.18 × 0.12 × 0.07 mm^3	
Theta range for data collection	1.39 to 27.49°.	
Index ranges	-14<=h<=14, -28<=k<=28, -26<=l<=25	
Reflections collected	54901	
Independent reflections	11248 [R(int) = 0.0520]	
Completeness to theta = 27.49°	98.9 %	
Max. and min. transmission	0.9309 and 0.8351	
Refinement method	Full-matrix least-squares on F^2	
Data / restraints / parameters	11248 / 1473 / 1196	
Goodness-of-fit on F^2	1.139	
Final R indices [I > 2sigma(I)]	R1 = 0.0959, wR2 = 0.2166	
R indices (all data)	R1 = 0.1132, wR2 = 0.2262	
Largest diff. peak and hole	1.194 and -0.880 e·$Å^{-3}$	

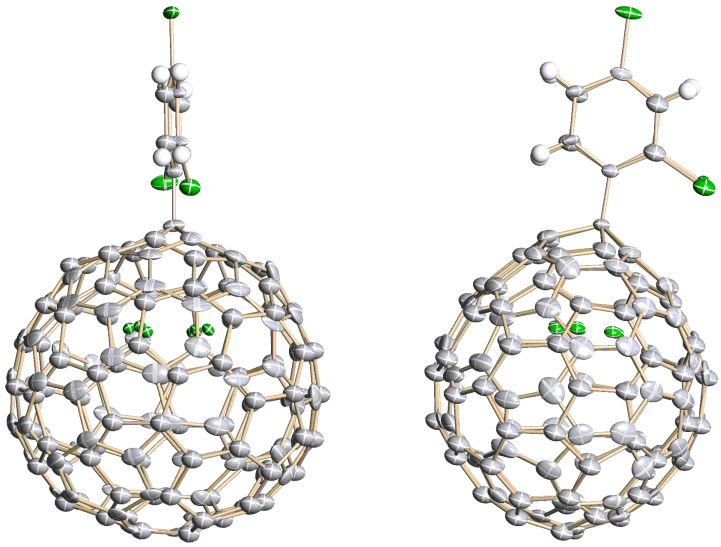

Figure S15. Two views of the crystal structures of La@$C_{80}(C_6H_3Cl_2)$(A).

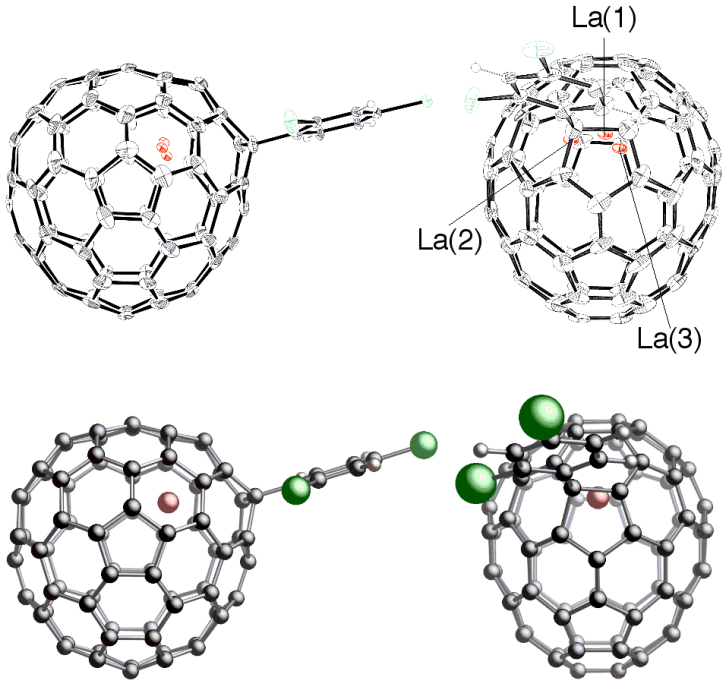

Figure S16. Two views of (a) the ORTEP drawing of one enantiomeric isomer of La@C_{80}($C_6H_3Cl_2$)(A) and (b) the optimized structure of La@C_{80}($C_6H_3Cl_2$)(A).

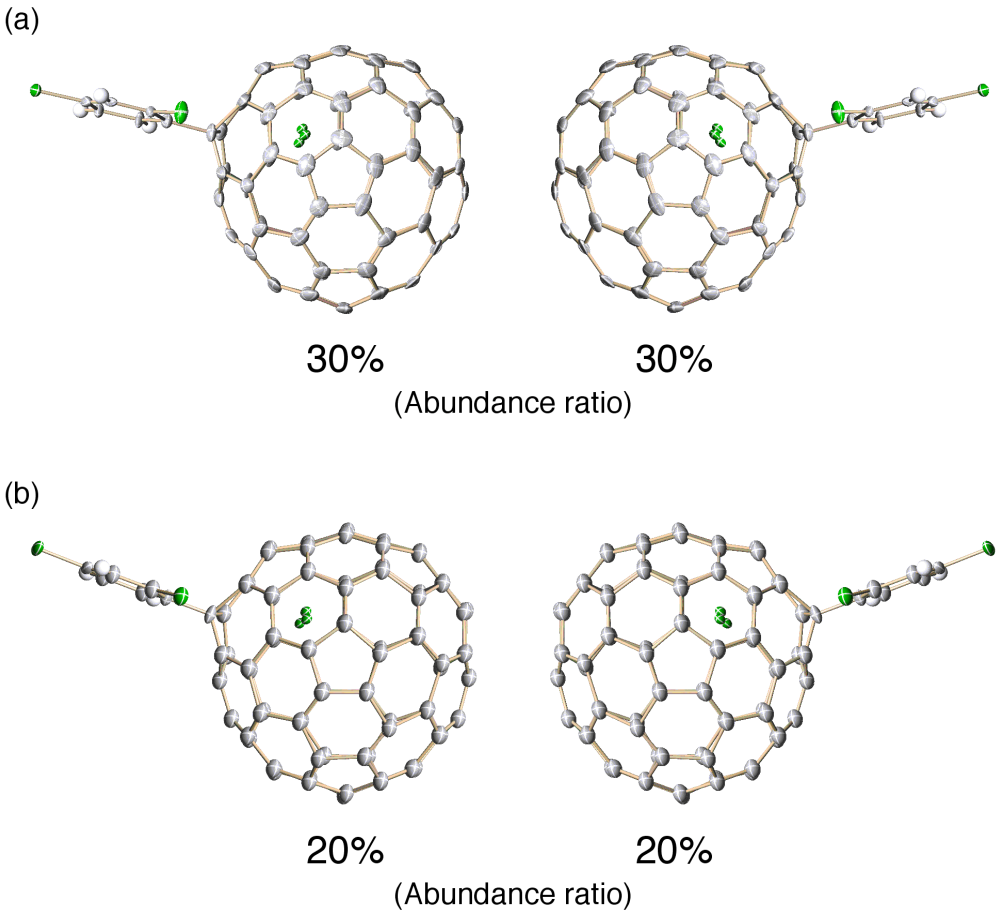

Figure S17. Crystal structure of (a) major and (b) minor enantiomeric isomers of La@C_{80}($C_6H_3Cl_2$)(A) at 90 K showing thermal ellipsoids at the 30% probability level.

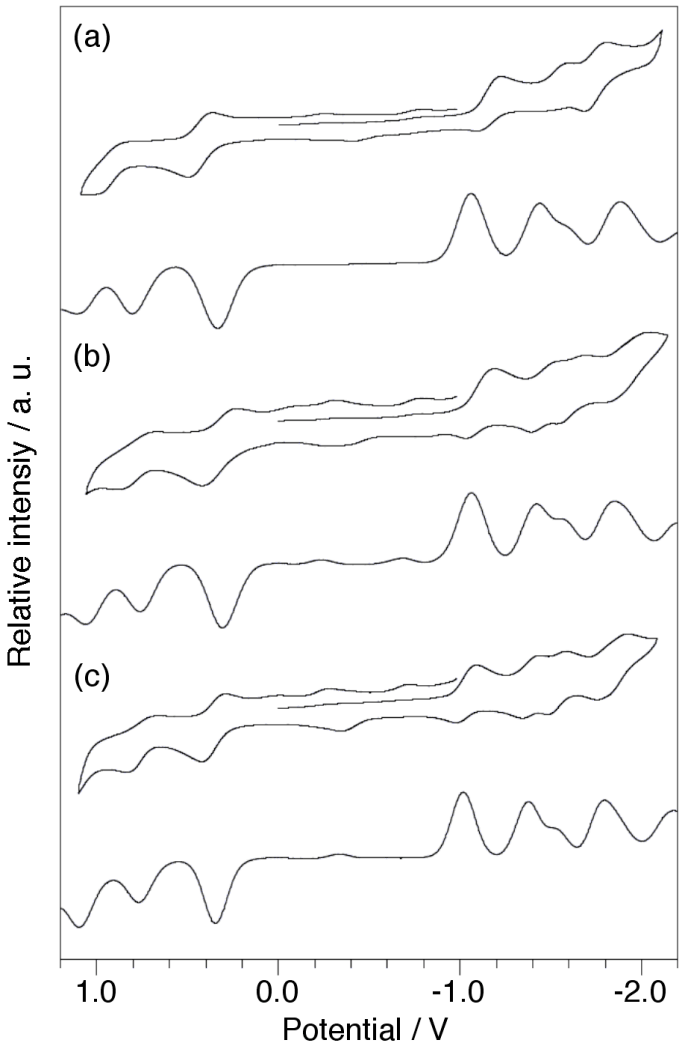

Figure S18. Cyclic and differential pulse voltammograms of (a) La@$C_{80}C_6H_3Cl_2$ (A), (b) La@$C_{80}C_6H_3Cl_2$ (B), and La@$C_{80}C_6H_3Cl_2$(C).

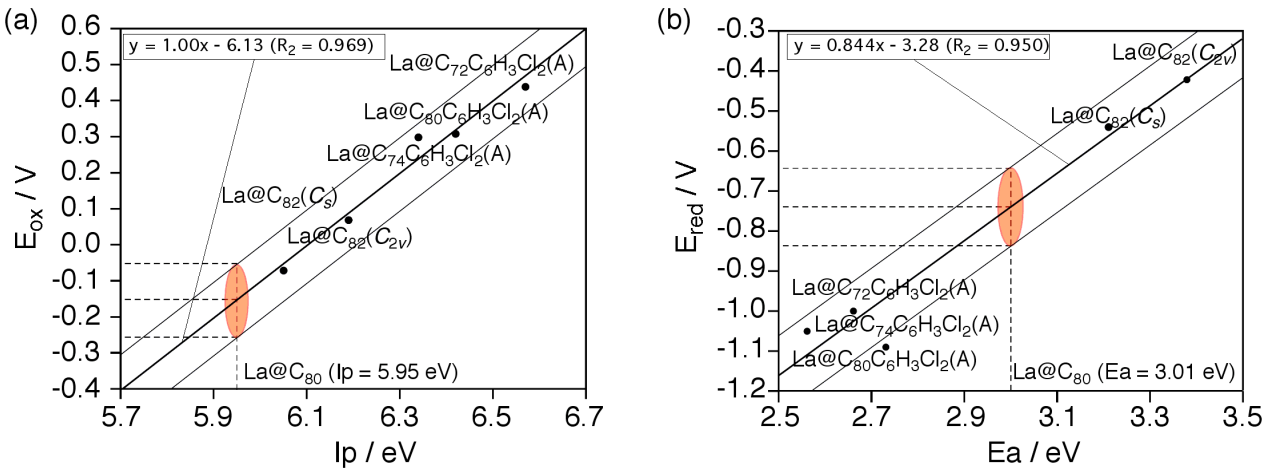

Figure S19. (a) Plot of oxidation potentials (E_{ox}) and ionization potentials (Ip) and (b) reduction potentials (E_{red}) and electron affinity (Ea) of La@$C_{72}C_6H_3Cl_2$(A), La@$C_{74}C_6H_3Cl_2$(A), La@$C_{80}C_6H_3Cl_2$(A), La@$C_{82}(C_{2v})$, and La@$C_{82}(C_s)$.

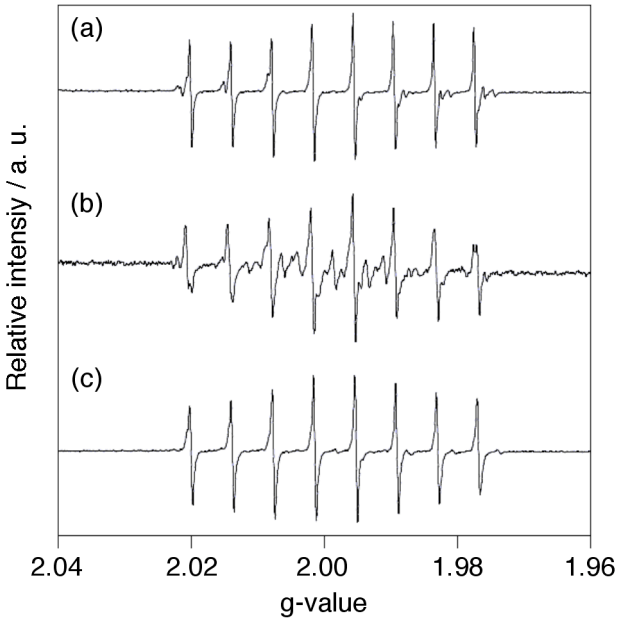

Figure S20. EPR spectra of the radical species formed by CV and DPV measurements of (a) La@$C_{80}C_6H_3Cl_2$(A), (b) La@$C_{80}C_6H_3Cl_2$(B), and (c) La@$C_{80}C_6H_3Cl_2$(C).